Development and in vivo efficacy of targeted polymeric inflammation-resolving nanoparticles

Nazila Kamaly[a,1], Gabrielle Fredman[b,1], Manikandan Subramanian[b], Suresh Gadde[a], Aleksandar Pesic[a], Louis Cheung[a], Zahi Adel Fayad[c], Robert Langer[d,2], Ira Tabas[b,2], and Omid Cameron Farokhzad[a,2]

[a]Laboratory of Nanomedicine and Biomaterials, Department of Anesthesiology, Brigham and Women's Hospital, Harvard Medical School, Boston, MA 02115; [b]Departments of Medicine, Pathology and Cell Biology, and Physiology, Columbia University, New York, NY 10032; [c]Translational and Molecular Imaging Institute, Mount Sinai School of Medicine, New York, NY 10029; and [d]Department of Chemical Engineering, Massachusetts Institute of Technology, Cambridge, MA 02139

Excessive inflammation and failed resolution of the inflammatory response are underlying components of numerous conditions such as arthritis, cardiovascular disease, and cancer. Hence, therapeutics that dampen inflammation and enhance resolution are of considerable interest. In this study, we demonstrate the proresolving activity of sub–100-nm nanoparticles (NPs) containing the anti-inflammatory peptide Ac2-26, an annexin A1/lipocortin 1-mimetic peptide. These NPs were engineered using biodegradable diblock poly(lactic-co-glycolic acid)-b-polyethyleneglycol and poly(lactic-co-glycolic acid)-b-polyethyleneglycol collagen IV–targeted polymers. Using a self-limited zymosan-induced peritonitis model, we show that the Ac2-26 NPs (100 ng per mouse) were significantly more potent than Ac2-26 native peptide at limiting recruitment of polymononu-clear neutrophils (56% vs. 30%) and at decreasing the resolution interval up to 4 h. Moreover, systemic administration of collagen IV targeted Ac2-26 NPs (in as low as 1 μg peptide per mouse) was shown to significantly block tissue damage in hind-limb ischemia-reperfusion injury by up to 30% in comparison with controls. Together, these findings demonstrate that Ac2-26 NPs are proresolving in vivo and raise the prospect of their use in chronic inflammatory diseases such as atherosclerosis.

nanomedicine | nanotechnology | controlled release | inflammation resolution

Acute inflammation is a protective response that combats invading organisms and repairs tissue injury (1). Ideally, this response is self-limited and leads to clearance of pathogens, cellular debris, and inflammatory mediators (1, 2). However, an excessive inflammatory response impairs resolution and leads to chronic inflammation and subsequent tissue damage (2–4). Increasing evidence suggests that excessive inflammation and impaired resolution play central roles in several prevalent diseases including cardiovascular, metabolic, and neurodegenerative diseases (5). Hence, development of therapeutics that temper inflammation and enhance resolution are of considerable interest (3, 4, 6).

Resolution programs are active endogenous counterregulatory processes that are orchestrated, in part, by specialized proresolving lipid mediators (SPMs) (4). Examples of SPMs include lipoxins, resolvins, protectins, maresins, and specific peptide mediators such as annexin A1 (4, 7). Bannenberg et al. introduced and defined quantitative resolution indices in vivo that allow for temporal regulation of leukocyte trafficking and chemical mediators within inflammatory exudates (8). These indices are the maximal neutrophil numbers that are present in the exudates (ψ_{max}), the time when ψ_{max} occurs (T_{max}), and the resolution interval from T_{max} to T_{50} (R_i)—i.e., the time that it takes for the number of polymorphonuclear neutrophils (PMNs) to reach half ψ_{max} (8). Importantly, these indices not only provide a quantitative measure of the specific actions of endogenous SPMs and peptides but also provide a means to investigate whether pharmacologic agents can enhance or impair resolution (9–11). In this regard, only a few

widely used therapeutics have been assessed for their impact in programmed resolution (9, 10, 12)

The application of nanotechnology to medicine (nanomedicine) is expected to have a profound impact on human health (13, 14). Nanoparticles (NPs) are an important class of nanomedicines, and many distinct NP platforms have been developed to successfully deliver bioactive molecules and imaging agents to sites of disease (15–19). Recently, SPMs incorporated into NPs derived from human PMNs were shown to limit acute inflammation, enhance resolution, and reduce joint damage (11). In this study, we investigated the delivery and bioactions of polymeric NPs encapsulating Ac2-26, an annexin A1 N-terminal 25 amino acid mimetic peptide that acts on the G-protein–coupled formyl peptide receptor, ALX/FPR2, which is also the receptor for lipoxin A4 (7, 20, 21). Ac2-26 exerts anti-inflammatory (22) and proresolving actions in vivo and was shown to be protective in several disease models, including myocardial ischemia-reperfusion injury (23), allergic inflammation (24), and endotoxin-induced cerebral inflammation (25).

Polymers are versatile building blocks for NP development as they can be custom-synthesized with unique biocompatibility and degradation properties (26). Their physicochemical properties can be easily manipulated, allowing for the development of self-assembled and customizable, controlled release therapeutic NPs (16, 27–29). We encapsulated Ac2-26 in targeted polymeric NPs to improve the pharmaceutical and pharmacological properties of Ac2-26 by enhancing its systemic circulation in vivo, site-specific delivery, and controlled release in a spatiotemporal manner. Additionally, we used a collagen IV (Col IV)-targeted heptapeptide ligand that we have previously identified by phage display (30). Because Col IV represents 50% of the vascular basement membrane, we hypothesized that Col IV exposure will occur at sites of vascular inflammation and injury (30, 31), enabling targeting of our NPs to sites of vascular injury. Here, we demonstrate that Ac2-26 NPs are proresolving in vivo and are significantly more potent than the Ac2-26 native peptide at blocking zymosan-stimulated PMN recruitment in an acute peritonitis model. Additionally, using a hind-limb ischemia-reperfusion model of vascular and tissue injury, we show that Col IV-targeted Ac2-26 NPs

MEDICAL SCIENCES

exert a tissue-restorative property. The proresolving targeted NPs developed in this study may prove beneficial for more chronic diseases in which excessive inflammation plays a critical role.
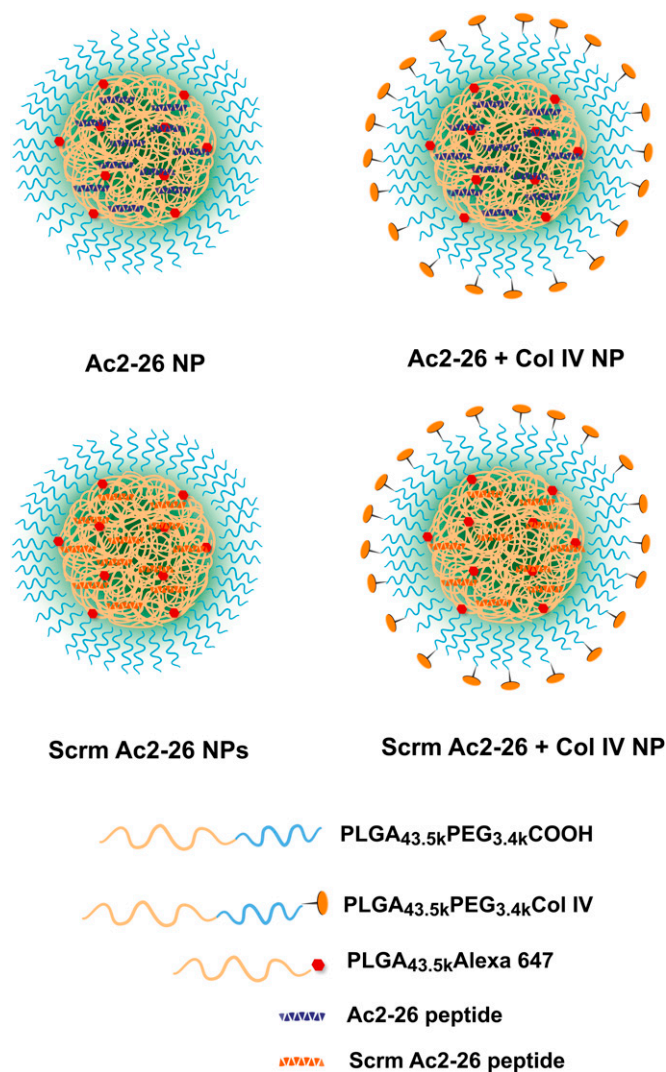
Results

Synthesis and Characterization of Targeted Ac2-26 Col IV NPs and Controls. The NPs were created via a single-step nanoprecipitation self-assembly method. In addition to nontargeted and Col IV-targeted Ac2-26 NPs, nontargeted and targeted NPs containing a randomly generated, isoelectric, mismatched scrambled sequence (Scrm Ac2-26) were also engineered (Fig. 1) to control for the biophysicochemical properties of the Ac2-26 peptide. In addition, some experiments used free Ac2-26 peptide in solution to compare

Fig. 1. Nanoparticle design and engineering. Nontargeted and targeted (Col IV) NPs encapsulating the Ac2-26 peptide or a randomly generated, isoelectric mismatched scrambled sequence (Scrm Ac2-26) were developed using biodegradable polymers via a single-step nanoprecipitation method. The synthesized polymers and Ac2-26 peptide or Scrm Ac2-26 peptide were dissolved in acetonitrile (total polymer 3 mg/mL), and 2% (wt/wt) of the fluorescent PLGA-Alexa 647 was added to all formulations. All NP samples contained 4% (wt/wt) peptide (either Ac2-26 or scrambled Ac2-26), and targeted NPs contained 5% (wt/wt) of the Col IV peptide-conjugated targeting polymer. The organic mixture containing the polymers and peptide was then added dropwise to nuclease-free water (10 mL). The solution was stirred for 2–4 h, and the particles were filtered, washed, and resuspended in water or PBS.

the additional anti-inflammatory benefits conferred by the encapsulation of Ac2-26 within NPs. To engineer polymeric NPs, copolymers of poly(lactic-*co*-glycolic acid)-*b*-polyethyleneglycol (PLGA-PEG) and Col IV peptide-conjugated PLGA-PEG-collagen IV–targeted polymers and a fluorescent polymer were synthesized according to Fig. S1. The carboxy terminal of PLGA and the amino functionality of PEG were coupled using 1-ethyl-3-(3-dimethylaminopropyl)carbodiimide hydrochloride (EDC) and *N*-hydroxysuccinimide (NHS) activation methodology to yield **1** (Fig. S1). The PLGA-PEG-COOH was then coupled to the heterobifunctional maleimide-PEG-hydroxy to yield PLGA-PEG-maleimide (PLGA-PEG-Mal) (**2**). The Col IV peptide-conjugated targeting polymer was then synthesized by conjugating the KLWVLPK peptide to PLGA-PEG-Mal via the free thiol of the C-terminal GGGC linker using maleimide chemistry. The product was purified and washed by precipitation in cold methanol to obtain **3** (Fig. S1). A fluorescent polymer was also synthesized by coupling carboxy terminated PLGA to Alexa 647 cadaverine to give polymer **4** (Fig. S1). With the polymers in hand, and characterized by 1H NMR (Figs. S2–S5), the NPs were engineered, purified, and characterized. The hydrodynamic size of the various NPs in water were as follows: empty NPs, 58.1 ± 0.8 nm; Ac2-26 NPs, 62.1 ± 0.8 nm; Ac2-26 Col IV NPs, 76.3 ± 0.9 nm; Scrm Ac2-26 NPs, 68.4 ± 0.7 nm; and Scrm Ac2-26 Col IV NPs, 77.15 ± 1.1 nm (Fig. 2*A*). The surface charge of the NPs were as follows: empty NPs, -21.55 ± 1.21 mV; Ac2-26 NPs, -28.77 ± 0.82 mV; Ac2-26 Col IV NPs, -19.68 ± 0.78 mV; Scrm Ac2-26 NPs, -30.71 ± 1.0 mV; and Scrm Ac2-26 Col IV NPs, -15.49 ± 0.84 mV (Fig. 2*B*). The Col IV-bearing NPs were larger than the nontargeted NPs ($\sim$8.75 nm for Ac2-26 Col IV NPs and $\sim$14.2 nm for Scrm Ac2-26 Col IV NPs) and were also more positive in charge ($\sim$9.09 and $\sim$15.22 mV, respectively). The increase in size is attributed to the increased bulk of the NPs bearing the Col IV-targeted peptide sequence, and the increase in positive charge may be due to the N-terminal exposed orientation of the peptide.
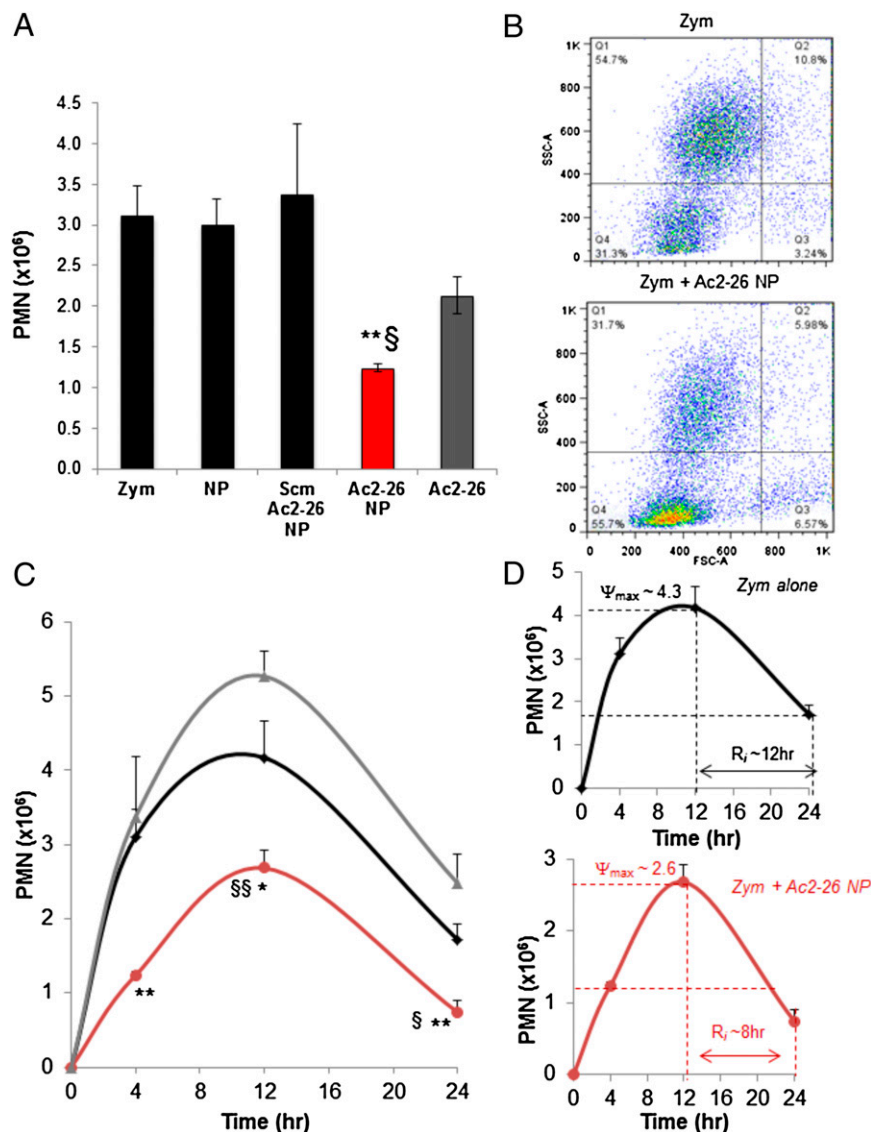
The peptide loading and release rates of the NPs were then measured. The loading of the peptide in the NPs was optimal up to 4% nominal loading (peptide/polymer wt/wt). At this ratio, the NPs were stable, and release could be optimally tuned. The size of the NPs was also kept at sub-100 nm for improved vessel adhesion and retention (32–35). The percentage encapsulation efficiency and loading were measured to be $\sim$90% and 3.36%, respectively, for peptide-loaded NPs. The Ac2-26 NPs were optimized for sustained release, i.e., for up to a period no longer than 1 wk to facilitate a single weekly dosing regimen for future studies using chronic inflammatory disease models. The release kinetics of Ac2-26 from targeted and nontargeted NPs was measured by incubating the NPs at 37 °C and then measuring the released peptide in solution, which was isolated via ultracentrifugation. Released peptide concentrations were measured using UV spectroscopy, and a cumulative release curve was generated (Fig. 2*C*). The release of Ac2-26 from the NPs was found to be $\sim$20% per day. Transmission electron microscopy (TEM) revealed that the targeted NPs were spherical and had uniform structure (Fig. 2*D*).

Proresolving Bioactions of Ac2-26 NPs in Vivo. To determine whether the developed NPs containing Ac2-26 are anti-inflammatory and/or proresolving, we used a model of self-limited peritonitis to quantitatively assess resolution in vivo (8, 9). C57BL/6J mice were administered 100 μg of zymosan i.p. per mouse. In parallel, mice were then given vehicle, empty NPs, 100 ng per mouse Ac2-26 in NPs, 100 ng per mouse Scrm Ac2-26 in NPs, or 100 ng per mouse Ac2-26 native peptide. Equal polymer concentration was loaded in both the NPs and the Ac2-26 NPs. Ac2-26 NPs blocked zymosan-stimulated PMN infiltration by $\sim$56% ($P < 0.01$), whereas freely administered Ac2-26 peptide blocked PMN infiltration by only $\sim$30%, which did not reach statistical significance (Fig. 3*A*). Empty

Kamaly et al.

Fig. 2. Characterization of polymeric NPs. (*A*) Dynamic light-scattering measurements of empty, nontargeted (Ac2-26 NP), targeted (Ac2-26 + Col IV NP), scrambled peptide (Scrm Ac2-26 NP), and targeted scrambled peptide (Scrm Ac2-26 + Col IV NP) NPs were measured (mean ± SD, $n = 3$). (*B*) ζ-Potential of the NPs in *A* were also measured. (*C*) In vitro cumulative release curve of Ac2-26 peptide from targeted and nontargeted NPs incubated at 37 °C is shown (mean ± SD, $n = 3$). The released peptide at different time points was isolated by filtration, and the absorbance of these samples was measured at 220 nm. (*D*) Representative TEM images of Ac2-26 Col IV NPs stained with 0.75% uranyl formate at 80 kV (98,000×). (Scale bar, 60 nm.)

NPs did not exert a protective effect, indicating that the pro-resolving action was a result of the Ac2-26 and not the polymeric composition of the NPs. The Ac2-26 scrambled peptide was also not protective, confirming that the specific sequence of Ac2-26 peptide confers protective action. Flow cytometric analysis of the peritoneal exudate cells showed that there were fewer PMNs in the Ac2-26 NP-treated group (Fig. 3*B*, *Lower*) vs. the zymosan-alone group (Fig. 3*B*, *Upper*).

Acute inflammation and its timely resolution are programmed temporal events (3, 36). In this regard, resolution can be defined at the histological level as the interval from maximum PMN infiltration to the point where PMNs are lost from the tissue (8). Zymosan exhibited a self-limited PMN curve with a maximal PMN infiltration (ψ_{max}) of ~4.3×10^6 PMNs, a T_{max} of 12 h (Fig. 3 *C* and *D*), and a resolution interval (R_i) of ~12 h (Fig. 3 *C* and *D*). The scrambled Ac2-26 peptide did not block zymosan-stimulated PMN infiltration at any time point. Notably, the free Ac2-26 peptide was not used here because it did not significantly limit PMN infiltration at the dose of 100 ng per mouse (Fig. 3*A*). Also, it is already known that native Ac2-26 peptide exerts anti-inflammatory actions and blocks PMN infiltration at higher doses in this model (22). In contrast, NPs containing Ac2-26 (100 ng per mouse) significantly blocked PMN infiltration at 4, 12, and 24 h post zymosan challenge and exhibited a ψ_{max} of ~2.6×10^6 PMNs, a T_{max} of 12 h, and a R_i of 8 h (Fig. 3 *C* and *D*). Thus, Ac2-26 NPs enhanced resolution 4 h faster than zymosan alone.

Tissue Restorative Bioactions of Targeted Ac2-26 Col IV NPs in Vivo. Excessive accumulation of PMN within tissues can lead to tissue damage, amplification, and prolongation of the inflammatory response (1). Because we showed that Ac2-26 NPs limit PMN infiltration in vivo (Fig. 3), we next sought to investigate the actions of Ac2-26 NPs in a model of tissue injury driven by excessive PMN infiltration and activation (37) (Fig. 4). In this regard, we chose a model of hind-limb ischemia reperfusion in which a tourniquet was tied around the hind limbs of the mice for 1 h to induce ischemia. After 1 h, the tourniquet was removed, and the mice were injected with vehicle, Ac2-26 NPs, Ac2-26 Col IV

NPs, or Scrm Ac2-26 Col IV NPs (each at 1 μg peptide or vehicle equivalent per mouse). After 1 h of reperfusion, the mice were euthanized, and the gastrocnemius muscle was harvested to assess local tissue damage. Col IV is abundant in basement membranes and is exposed upon injury (30, 31), and so we hypothesized that the targeted NPs would home to the site of injury and release Ac2-26 more efficiently than the nontargeted NPs. Indeed, Ac2-26 Col IV NPs differentially localized to the injured tissue, compared with nontargeted Ac2-26 NPs (Fig. 4*A*). Also, Ac2-26 Col IV NPs limited PMN infiltration by ~30%, whereas Ac2-26 NPs or Scrm Ac2-26 Col-IV NPs had no inhibitory effect (Fig. 4*B*). Thus, Ac2-26 Col IV NPs displayed a restorative action in this model of tissue injury after only 1 h of postsystemic administration.

Discussion

Failed resolution of inflammation is the underlying component in several prevalent diseases, and thus development of therapeutics that enhance resolution are of considerable interest (3). In the present report, we investigated the delivery and bioactions of polymeric NPs containing the anti-inflammatory Ac2-26 peptide. Our results demonstrate that Ac2-26 NPs can be encapsulated successfully in sub–100-nm NPs, exhibit controlled temporal release, and exert potent proresolving actions in vivo, indicating that they enhance endogenous resolution programs.

The polymeric NP design used in this study incorporated biocompatible, biodegradable, and bioeliminable materials and made use of a self-assembly approach. Conventional methods of engineering targeted NPs involve a series of synthetic coupling steps involving the bioconjugation of targeting ligands to the surface of preformed NP cores (26). This postcoupling of targeting ligands requires excessive amounts of reagents to achieve high coupling efficiencies and requires further NP purification techniques to remove unbound ligands. As such, heterogeneity may arise in the reproducibility of NP surface properties and ligand densities, resulting in batch-to-batch variability, which may hinder successful clinical translation and subsequent commercialization (26). The design of prefunctionalized peptide-conjugated copolymers allows for the reproducible creation of optimal targeted NPs, whereby

Fig. 3. Ac2-26 NPs are more potent than Ac2-26 and are proresolving in vivo. Zymosan (100 μg per mouse) was administered i.p., followed by i.v. injections of vehicle, empty NPs, or NPs containing Ac2-26 (Ac2-26 NP, 100 ng per mouse), scrambled Ac2-26 (Scrm Ac2-26 NP, 100 ng per mouse), or Ac2-26 native peptide (100 ng per mouse). Peritoneal exudates were harvested 4 h post zymosan initiation, and living cells were quantified using trypan blue exclusion. (*A*) PMNs were assessed by flow cytometry (*n* = 3; mean ± SEM). **$P < 0.01$ for zymosan vs. treatment; §$P < 0.05$ for Ac2-26 NP versus Ac2-26. (*B*) Representative dot plot of exudate cells. (*Upper*) Zymosan alone. (*Lower*) NP-treated group. (*C*) Peritoneal exudates were harvested 4, 12, and 24 h post zymosan treatment, and PMNs were enumerated (Scrm Ac2-26 NPs, gray; vehicle, black; Ac2-26 NPs, red). *$P < 0.05$, **$P < 0.01$ for zymosan vs. Ac2-26 NPs; §$P < 0.05$ for Ac2-26 NP vs. Scrm Ac2-26; §§$P < 0.01$. (*D*) Resolution indices for zymosan alone (*Upper*) and Ac2-26 NPs (*Lower*) (*n* = 3; mean ± SEM).

controlling the self-assembly and ratio of each constituent can lead to targeted polymeric NPs with precisely tuned biophysicochemical properties (29). The use of diblock hydrophobic-PEGylated polymers in nanoprecipitation leads to NPs that consist of a hydrophobic core, with entrapped therapeutics surrounded by a hydrophilic PEG shell for steric stabilization and prolonged systemic circulation (38). In nanoprecipitation, the instantaneous formation of particles is governed by the principles of the Marangoni effect and has been attributed to interfacial interactions between liquid phases (39). Nanoprecipitation is a simple method, amenable to scale-up at an industrial scale, and requires only mild mixing under minimal sheer stress. In general, smaller NPs are obtained through this method compared with other methods under equivalent conditions.

The Ac2-26 NPs enhanced resolution 4 h sooner than vehicle treatment, underscoring their proresolving actions (Fig. 3*D*). Resolution of inflammation is a highly complex process and

involves a delicate balance of pro- and anti-inflammatory mediators (8, 36, 40). Several reports from the literature indicate therapeutics that either impair or enhance resolution (as reviewed in ref. 3). For example, cyoclooxygenase and lipoxygenase inhibitors (9) and lidocaine (10) impair resolution. The most notable drugs that impair resolution are the COX-2 inhibitors that block the production of PGE_2 and PGD_2, two critical mediators that initiate resolution (41). On the other hand, aspirin or glucoroticoids enhance resolution via the generation of aspirin-triggered SPMs (3) or by the endogenous production of annexin-A1, respectively (42). Furthermore, SPMs and annexin-A1 bind specific receptors and serve as agonists that trigger protective mechanisms and promote the return to homeostasis (36, 42). Restoring tissue homeostasis is vital in resolution (36). In this regard, the tissue-targeted Col-IV Ac2-26 NPs produced an ~30% inhibition of PMN infiltration into the damaged gastrocenemius (Fig. 4). Because PMNs can also
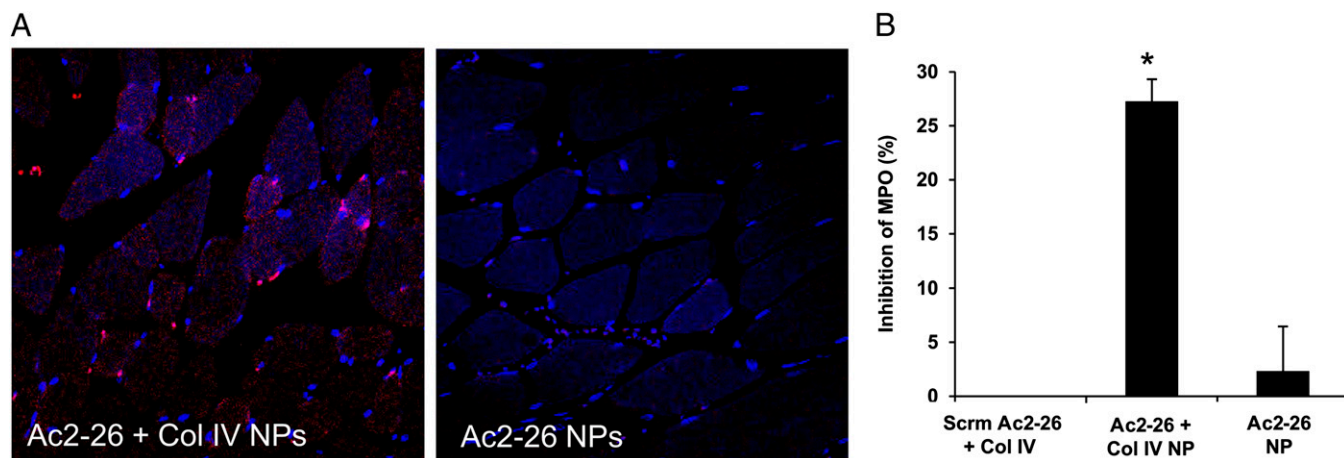
Fig. 4. Col–IV–targeted Ac2-26 NPs limit PMN infiltration into injured tissue. Ischemia was induced by placing a tourniquet around the hind limb for 1 h. After 1 h, the tourniquet was released and vehicle, Scrm Ac2-26 Col-IV NPs, Ac2-26 Col-IV NPs, or Ac2-26 NPs were injected i.v. Reperfusion was carried out for 1 h. The gastroconemius muscle tissue was harvested and (*A*) sectioned for confocal imaging using a Nikon A1R microscope, 20× magnification. Images are representative of *n* = 3. (*B*) Gastroconemius tissue was lysed and homogenized to assess PMNs using an MPO ELISA (*n* = 3; mean ± SEM). The data are plotted as inhibition of tissue MPO. *$P < 0.05$ Col-IV for Ac2-26 NPs vs. Ac2-26 NPs or vs. Scrm-Ac2-26 Col-IV–targeted NPs.

have protective and restorative actions in this model, complete inhibition would be detrimental to the overall resolution of tissue inflammation (43), underscoring the fact that tempering acute inflammation, rather than blocking it, is an optimal intervention. As predicted, the Scrm Ac2-26 NPs, which served as an important control for the biophysicochemical properties of Ac2-26 NPs, did not exert anti-inflammatory or proresolving actions (Figs. 2 and 3). Thus, it is the specific sequence and structure of the native Ac2-26 peptide that confers its anti-inflammatory and proresolving properties. Results presented here are in agreement with current literature that indicates a tissue-protective role for Ac2-26 in myocardial (23) and renal ischemia-reperfusion injury (44). Notably, these studies used Ac2-26 at a much higher microgram dose range, whereas Ac2-26 encapsulated in NPs in this study is protective against hind-limb ischemia-reperfusion injury in as low as 1 µg per mouse (Fig. 4).

Conclusions

In summary, we have developed targeted biodegradable polymeric NPs capable of releasing the anti-inflammatory annexin A1/lipocortin A1 mimetic peptide Ac2-26 in a spatiotemporal manner. These NPs were shown to enhance resolution in vivo and blunt excessive inflammation in a hind-limb ischemia-reperfusion model. These proresolving NPs have potential for treatment of a wide array of diseases such as atherosclerosis, where excessive inflammation is an underlying pathology.

Materials and Methods

See *SI Materials and Methods* for detailed materials and methods. Detailed descriptions of the synthesis and characterization of all compounds can be found in *SI Materials and Methods*.

Development and Characterization of NPs. The required polymers (3.12 mg/mL, 3 mg polymer + 120 µg Ac2-26 peptide) and Ac2-26 or Scrm Ac2-26 (0.12 mg/mL) were dissolved in acetonitrile. All NPs contained 4% (wt/wt) peptide (either Ac2-26 or Scrm Ac2-26) and targeted NPs contained 5% (wt/wt) of the PLGA-PEG-Col IV–targeting polymer. The polymer/peptide mixture was then added dropwise to 10 mL of nuclease-free water. The NPs were stirred for 2 h and filtered through sterile 0.45-µm syringe filters (regenerated cellulose, 17 mm; Cole Palmer Instruments). The NPs were concentrated by centrifugation at 3,000 × *g* for 20 min using Amicon Ultra-15 centrifugal filter units (MWCO 100 kDa; Sigma-Aldrich), washed with deionized water, and resuspended in 1 mL of either nuclease-free H₂O or PBS (total 3.12 mg/mL NP). For in vivo studies, NPs were resuspended in 1 mL of H₂O (total 3.12 mg/mL NP) and then further diluted with PBS before injection. The NPs were diluted 20-fold in either H₂O or PBS, and their size and surface charge were measured using dynamic light

scattering. For TEM, a 10-µL solution of 1 mg/mL freshly prepared NPs in H₂O was deposited on carbon-coated copper grids, the excess solution was blotted, and the grids were immersed in a solution of 0.75% uranyl formate stain. The stain was blotted, and the dried grids imaged within 1 h of preparation on a Tecnai G² Spirit BioTWIN electron microscope equipped with an AMT 2k CCD camera and low-dose software (80 kV, direct magnification of 98,000×). A calibration curve of various concentrations of the Ac2-26 or scrambled Ac2-26 peptide was also generated to quantify the amount of peptide retained in the NP samples. The absorbance of the initial filtrate was measured at 220 nm, and the percentage of encapsulation efficiency and percentage of loading of the peptides were calculated. Peptide loading is defined as the mass fraction of peptide in the NPs, whereas encapsulation efficiency is the fraction of initial drug that is encapsulated by the NPs.

Ac2-26 NP Release Kinetics Study. To quantify the Ac2-26 release profile, 3.12 mg/mL NP samples were made in PBS, and the NPs were incubated in Eppendorfs in triplicate at 37 °C. At defined time intervals (8, 24, 48, 72, and 96 h), the NPs were removed, transferred to Amicon Ultra-15 centrifugal filter units (MWCO 10 kDa; Sigma-Aldrich), and centrifuged at 3,000 × *g* for 20 min. The NPs were then resuspended in PBS, and incubation was continued until the designated time point. The filtrate (10 µL) was analyzed with a nanodrop UV-Vis spectrometer, and absorbance was measured at 220 nm to determine the amount of released peptide at each time point.

In Vivo Murine Peritonitis. Female C57BL/6J mice (6–8 wk old; Charles River Laboratories) were administered i.p. with zymosan A (100 µg per mouse; Sigma-Aldrich, St. Louis) to induce peritonitis (8, 11), followed by i.v. injections of vehicle, empty NPs, NPs containing Ac2-26 (Ac2-26 NP, 100 ng per mouse) or Scrm Ac2-26 (Scrm Ac2-26 NP, 100 ng per mouse), or Ac2-26 native peptide (100 ng per mouse). Peritoneal exudates were harvested 4, 12, or 24 h post zymosan initiation, and cells were quantified using trypan blue exclusion. Differential cell counts were assessed via flow cytometry using an LSRII flow cytometer. Cells were stained with FITC-conjugated rat anti-mouse Ly-6G (clone 1A8) or rat IgG2c,κ isotype control. All procedures were conducted in accordance with protocols approved by the Columbia University Standing Committee on Animals guidelines for animal care.

Hind-Limb Ischemia Reperfusion Injury. Hind-limb ischemia was initiated using rubber-band tourniquets placed on each hind limb as described previously (37). Mice were subjected to hind-limb ischemia for 1 h, after which the tourniquets were removed to initiate reperfusion. At the time of reperfusion, mice were administered 1 µg i.v. of Col-IV–targeted Ac2-26 NPs, Ac2-26 NPs, Col IV-targeted Scrm Ac2-26 NPs, or vehicle alone. At the end of this reperfusion period (1 h), the mice were euthanized with an overdose of anesthetic, and the gastrenemius was quickly harvested, placed in cold lysis buffer, and homogenized. Tissue levels of myeloperoxidase (MPO) in the resulting supernatants were determined using a mouse MPO ELISA (Hycult Biotech and Cell Sciences).

1. Majno G, Joris I (2004) *Cells, Tissues, and Disease: Principles of General Pathology* (Oxford Univ Press, New York), 2nd Ed, p xxviii, 1005 pp.
2. Medzhitov R (2010) Inflammation 2010: New adventures of an old flame. *Cell* 140(6): 771–776.
3. Serhan CN, et al. (2007) Resolution of inflammation: State of the art, definitions and terms. *FASEB J* 21(2):325–332.
4. Serhan CN (2010) Novel lipid mediators and resolution mechanisms in acute inflammation: To resolve or not? *Am J Pathol* 177(4):1576–1591.
5. Nathan C, Ding A (2010) Nonresolving inflammation. *Cell* 140(6):871–882.
6. Tabas I, Glass CK (2013) Anti-inflammatory therapy in chronic disease: Challenges and opportunities. *Science* 339(6116):166–172.
7. Perretti M, D'Acquisto F (2009) Annexin A1 and glucocorticoids as effectors of the resolution of inflammation. *Nat Rev Immunol* 9(1):62–70.
8. Bannenberg GL, et al. (2005) Molecular circuits of resolution: Formation and actions of resolvins and protectins. *J Immunol* 174(7):4345–4355.
9. Schwab JM, Chiang N, Arita M, Serhan CN (2007) Resolvin E1 and protectin D1 activate inflammation-resolution programmes. *Nature* 447(7146):869–874.
10. Chiang N, et al. (2008) Anesthetics impact the resolution of inflammation. *PLoS One* 3(4):e1879.other.
11. Norling LV, et al. (2011) Cutting edge: Humanized nano-proresolving medicines mimic inflammation-resolution and enhance wound healing. *J Immunol* 186(10):5543–5547.
12. Navarro-Xavier RA, et al. (2010) A new strategy for the identification of novel molecules with targeted proresolution of inflammation properties. *J Immunol* 184(3): 1516–1525.
13. Farokhzad OC, Langer R (2009) Impact of nanotechnology on drug delivery. *ACS Nano* 3(1):16–20.
14. Kamaly N, Xiao Z, Valencia PM, Radovic-Moreno AF, Farokhzad OC (2012) Targeted polymeric therapeutic nanoparticles: Design, development and clinical translation. *Chem Soc Rev* 41(7):2971–3010.
15. Farokhzad OC, et al. (2004) Nanoparticle-aptamer bioconjugates: A new approach for targeting prostate cancer cells. *Cancer Res* 64(21):7668–7672.
16. Farokhzad OC, et al. (2006) Targeted nanoparticle-aptamer bioconjugates for cancer chemotherapy in vivo. *Proc Natl Acad Sci USA* 103(16):6315–6320.
17. Hrkach J, et al. (2012) Preclinical development and clinical translation of a PSMA-targeted docetaxel nanoparticle with a differentiated pharmacological profile. *Sci Transl Med* 4(128):128ra139.
18. Xiao Z, et al. (2012) DNA self-assembly of targeted near-infrared-responsive gold nanoparticles for cancer thermo-chemotherapy. *Angew Chem Int Ed Engl* 51(47): 11853–11857.
19. Salvador-Morales C, Valencia PM, Gao W, Karnik R, Farokhzad OC (2012) Spontaneous formation of heterogeneous patches on polymer-lipid core-shell particle surfaces during self-assembly. *Small* 9(4):511–517.
20. Dufton N, et al. (2010) Anti-inflammatory role of the murine formyl-peptide receptor 2: Ligand-specific effects on leukocyte responses and experimental inflammation. *J Immunol* 184(5):2611–2619.
21. Perretti M, et al. (2002) Endogenous lipid- and peptide-derived anti-inflammatory pathways generated with glucocorticoid and aspirin treatment activate the lipoxin A4 receptor. *Nat Med* 8(11):1296–1302.
22. Perretti M, Getting SJ, Solito E, Murphy PM, Gao JL (2001) Involvement of the receptor for formylated peptides in the in vivo anti-migratory actions of annexin 1 and its mimetics. *Am J Pathol* 158(6):1969–1973.
23. La M, et al. (2001) Annexin 1 peptides protect against experimental myocardial ischemia-reperfusion: Analysis of their mechanism of action. *FASEB J* 15(12):2247–2256.
24. Bandeira-Melo C, et al. (2005) A novel effect for annexin 1-derived peptide ac2-26: Reduction of allergic inflammation in the rat. *J Pharmacol Exp Ther* 313(3):1416–1422.
25. Gavins FN, et al. (2012) Leukocyte recruitment in the brain in sepsis: involvement of the annexin 1-FPR2/ALX anti-inflammatory system. *FASEB J* 26(12):4977–4988.
26. Evans HL, et al. (2012) Copper-free click: A promising tool for pre-targeted PET imaging. *Chem Commun (Camb)* 48(7):991–993.
27. Makadia HK, Siegel SJ (2011) Poly lactic-co-glycolic acid (PLGA) as biodegradable controlled drug delivery carrier. *Polymers (Basel)* 3(3):1377–1397.
28. Chan JM, Valencia PM, Zhang L, Langer R, Farokhzad OC (2010) Polymeric nanoparticles for drug delivery. *Methods Mol Biol* 624:163–175.
29. Gu F, et al. (2008) Precise engineering of targeted nanoparticles by using self-assembled biointegrated block copolymers. *Proc Natl Acad Sci USA* 105(7):2586–2591.
30. Chan JM, et al. (2010) Spatiotemporal controlled delivery of nanoparticles to injured vasculature. *Proc Natl Acad Sci USA* 107(5):2213–2218.
31. Kalluri R (2003) Basement membranes: Structure, assembly and role in tumour angiogenesis. *Nat Rev Cancer* 3(6):422–433.
32. Fishbein I, et al. (2001) Formulation and delivery mode affect disposition and activity of tyrphostin-loaded nanoparticles in the rat carotid model. *Arterioscler Thromb Vasc Biol* 21(9):1434–1439.
33. Decuzzi P, Ferrari M (2006) The adhesive strength of non-spherical particles mediated by specific interactions. *Biomaterials* 27(30):5307–5314.
34. Westedt U, et al. (2002) Deposition of nanoparticles in the arterial vessel by porous balloon catheters: Localization by confocal laser scanning microscopy and transmission electron microscopy. *AAPS PharmSci* 4(4):E41.
35. Rothenfluh DA, Bermudez H, O'Neil CP, Hubbell JA (2008) Biofunctional polymer nanoparticles for intra-articular targeting and retention in cartilage. *Nat Mater* 7(3): 248–254.
36. Serhan CN, Chiang N, Van Dyke TE (2008) Resolving inflammation: Dual anti-inflammatory and pro-resolution lipid mediators. *Nat Rev Immunol* 8(5):349–361.
37. Qiu FH, Wada K, Stahl GL, Serhan CN (2000) IMP and AMP deaminase in reperfusion injury down-regulates neutrophil recruitment. *Proc Natl Acad Sci USA* 97(8): 4267–4272.
38. Mora-Huertas CE, Fessi H, Elaissari A (2010) Polymer-based nanocapsules for drug delivery. *Int J Pharm* 385(1–2):113–142.
39. Quintanar-Guerrero D, Allémann E, Fessi H, Doelker E (1998) Preparation techniques and mechanisms of formation of biodegradable nanoparticles from preformed polymers. *Drug Dev Ind Pharm* 24(12):1113–1128.
40. Fredman G, Li Y, Dalli J, Chiang N, Serhan CN (2012) Self-limited versus delayed resolution of acute inflammation: Temporal regulation of pro-resolving mediators and microRNA. *Sci Rep* 2:639.
41. Levy BD, Clish CB, Schmidt B, Gronert K, Serhan CN (2001) Lipid mediator class switching during acute inflammation: Signals in resolution. *Nat Immunol* 2(7): 612–619.
42. Perretti M, Dalli J (2009) Exploiting the Annexin A1 pathway for the development of novel anti-inflammatory therapeutics. *Br J Pharmacol* 158(4):936–946.
43. Muhs BE, Gagne P, Plitas G, Shaw JP, Shamamian P (2004) Experimental hindlimb ischemia leads to neutrophil-mediated increases in gastrocnemius MMP-2 and -9 activity: A potential mechanism for ischemia induced MMP activation. *J Surg Res* 117(2): 249–254.
44. Facio FN, Jr., et al. (2011) Annexin 1 mimetic peptide protects against renal ischemia/reperfusion injury in rats. *J Mol Med (Berl)* 89(1):51–63.